World Conference on Timber Engineering Oslo 2023

LOADING TEST OF CLT-SHEAR WALL CONNECTED WITH STEEL BAR－TIMBER COMPOSITE COLUMN DISSIPATING HIGH-ENERGY

Takumi Suyama [1], Riko Kawasaki [2], Atsuya Kawasoe[3], Tomokazu Yoshioka[4], Shinichi Shioya[5]

ABSTRACT: In light of the current climate crisis, there has been much recent interest in using timber structural members in large buildings, since timber is as renewable natural resource. Moreover, in severe earthquake prone zones, such as Japan, they are more desired on the grounds of light weight of timber members. We are developing a frame system formed by steel bar-timber composite members strengthened by deformed steel bars (i.e., rebars) using epoxy resin adhesive. We are also developing Cross Laminated Timber (CLT)-shear wall for the frame. One of the most excellent mechanical characteristics of CLT are its high shear stiffness and shear capacity. It is most advisable to use one long CLT panel as one continuous wall without cutting it at floor levels. This paper reports the application of the rotating shear plate concept to the CLT wall and experiment of the shear wall dissipating high-energy, by damper installed in a frame consisting of steel bar-timber composite columns and timber beams.

KEYWORDS: Shear wall, Cross-Laminated Timber, Composite timber, Column, Re-centering, Energy-dissipation

1 INTRODUCTION

One of the most excellent mechanical characteristics of Cross Laminated Timber (CLT) is its high shear stiffness and shear capacity. The structural component that can take advantage of that is shear wall. However, it is difficult to utilize fully the characteristics of CLTs, if they are cut and connected at floor level of each story in buildings, and they are also time-consuming and expensive. It is most advisable to use one long CLT panel as one continuous wall. The maximum dimension of one CLT panel available in Japan is 3.0 m x 12.0 m. It is possible to adopt the CLT as one 2-story to 4-story continuous wall. A mechanism is required to transfer the horizontal inertia force generated by the CLT slab during an earthquake to the shear wall. However, if the continuous wall yields in bending or rotates at its wall bottom, rotation, vertical misalignment deformation will occur at the connection between the slab and the wall above the second story. When the deformations are larger, it is currently difficult to transfer shear force between the slab and wall CLTs without damaging the connection during an earthquake. Future seismic design of buildings, on the other hand, will require performance to control damage and residual deformation. To control damage in slab-to-wall joints, a joint method that can only transmit horizontal shear force without restricting the rotation and the vertical deformation is desirable. Shioya has devised a shear key plate (rotational shear key) that allows rotation and transmits only shear forces in steel bar-timber composite column-beam connection [1]. Rocking wall is effective in reducing its residual deformation. Rocking CLT shear walls have already been developed [2], but the level of shear force that can be transmitted is extremely low, approximately 25% of the shear capacity of CLT wall. This paper reports the application of the rotational shear key plate concept to CLT shear wall and experiment of a shear wall dissipating high-energy by dampers, which are installed in a frame consisting of steel bar-timber composite columns and timber beams.

2 ARRANGEMENT AND AIM OF SHEAR WALL

Figure 1 shows a schematic diagram of assumed structure and shear wall, and its arrangement, where 3-story rigid-frame structure is assumed. Shear walls are placed in ridge direction. One-piece type of one CLT panel with a width of 3 m per one span (one-piece type) or two-piece type of two CLT panels can be assumed. Column is to be made of steel bar-timber composite column. The span in the ridge direction of building is assumed to be 3.6-3.8m and are connected with Glued laminated (Glulam) timber beams. The shear wall is assumed not to resist to axial forces from Dead load and Live load of building. Long-term loads are assumed to be resisted by the left and right columns of the shear wall.

The rotational shear key plate is incorporated so that its wall bottom performs as pin and is connected to RC foundation.

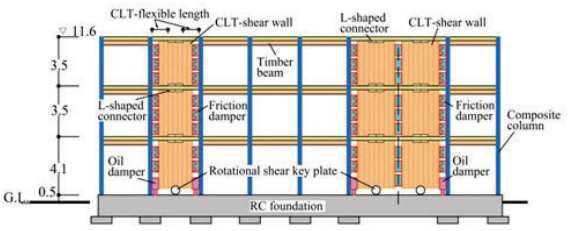

Figure 1: *Shear wall, damper, and rotational shear-key plate in a frame*

[1] Takumi Suyama, Department of Architecture, Kagoshima University, Japan
[2] Riko Kawasaki, Department of Architecture, Kagoshima University, Japan
[3] Atsuya Kawasoe, National institute of technology Kagoshima college, Japan
[4] Tomokazu Yoshioka, Kyusyu University, Japan
[5] Shinichi Shioya, Department of Architecture, Kagoshima University, Japan, k7347039@kadai.jp

https://doi.org/10.52202/069179-0451

Shear wall and CLT slab are connected to each other with L-shaped angle steel and screws (hereinafter referred to as "L-shaped hardware joint") only over center segment of the span.

As the slab is not restrained by the shear wall over section between the L-shaped hardware joint and its columns, the slab is expected to absorb the vertical deformation between the CLT wall and the columns and not to be damaged over the section.

Friction dampers and oil dampers are installed between the CLT wall and the column, dissipating energy using the vertical deformation between them which is caused by the rotation of the CLT wall. The friction damper is expected to dissipate vibration energy mainly during big earthquakes, i.e., after 1/200 rad. and the oil damper is expected to dissipate the vibration energy during frequent small and medium earthquakes and vibrations caused by wind loads to improve the habitability in building.

3 FRICTION DAMPER AND ITS PROPERTY

The shape of the damper is shown in Figure 2. It consists of a steel plate/Part A, T-shaped steel/Part B, two ultra-high strength aluminium plate/Part C for sliding material, two filler steel plate/Part D, two splice plates/ Part E, two thick square washer/Part F and a high-strength bolt/Part G. In the experiment, high-strength bolts with an embedded foil strain gauge were used to accurately measure tension force of the bolts. Part A is inserted into a slit cut in the

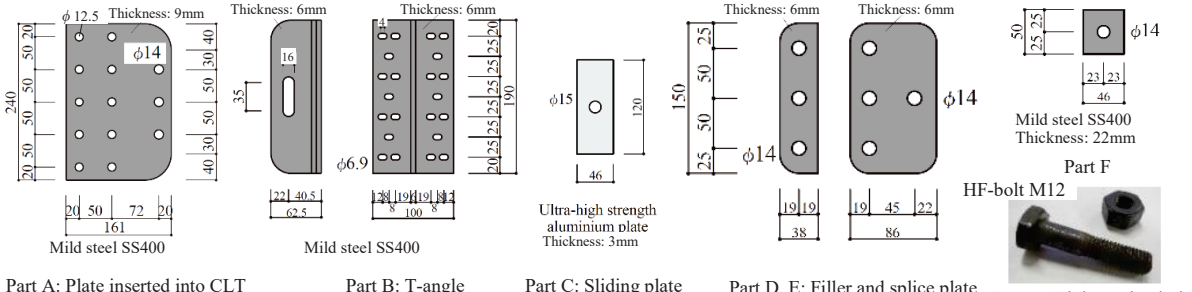

Figure 2: *Parts of proposed friction damper*

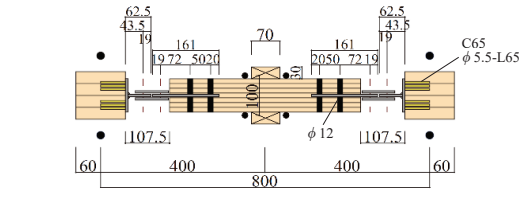

Photo 1: *PC steel bar embedded with a foil strain gauge ϕ 13-M14, Grade: C, Capacity:146^{kN}*

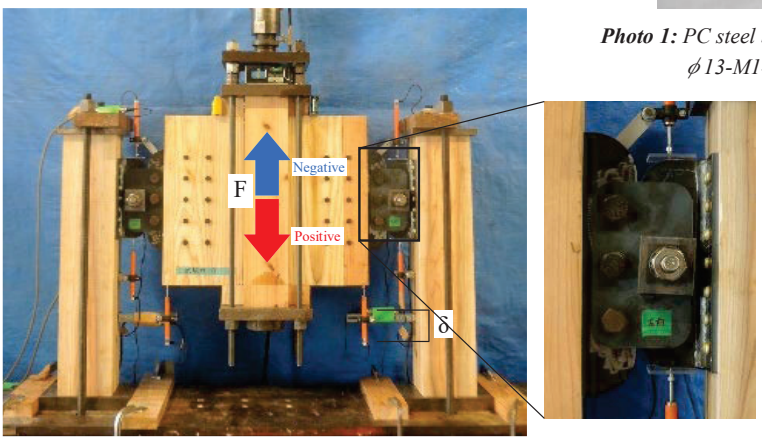

(a) Set-up for loading

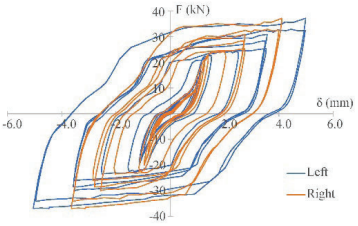

(b) Slip of overall

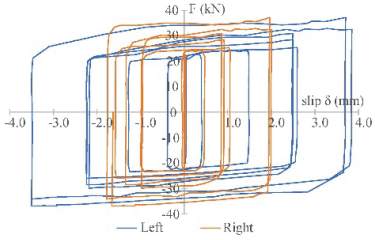

(c) Slip of Plate A – T-angle

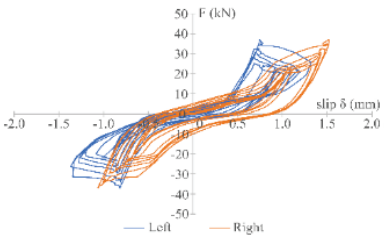

(d) Slip of CLT– Plate A

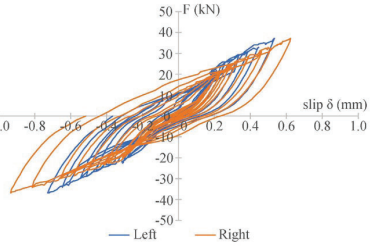

(e) Slip of T-angle–column

Figure 3: *Damper specimen and Vertical force/F-slip deformation/ δ relationships*

https://doi.org/10.52202/069179-0451

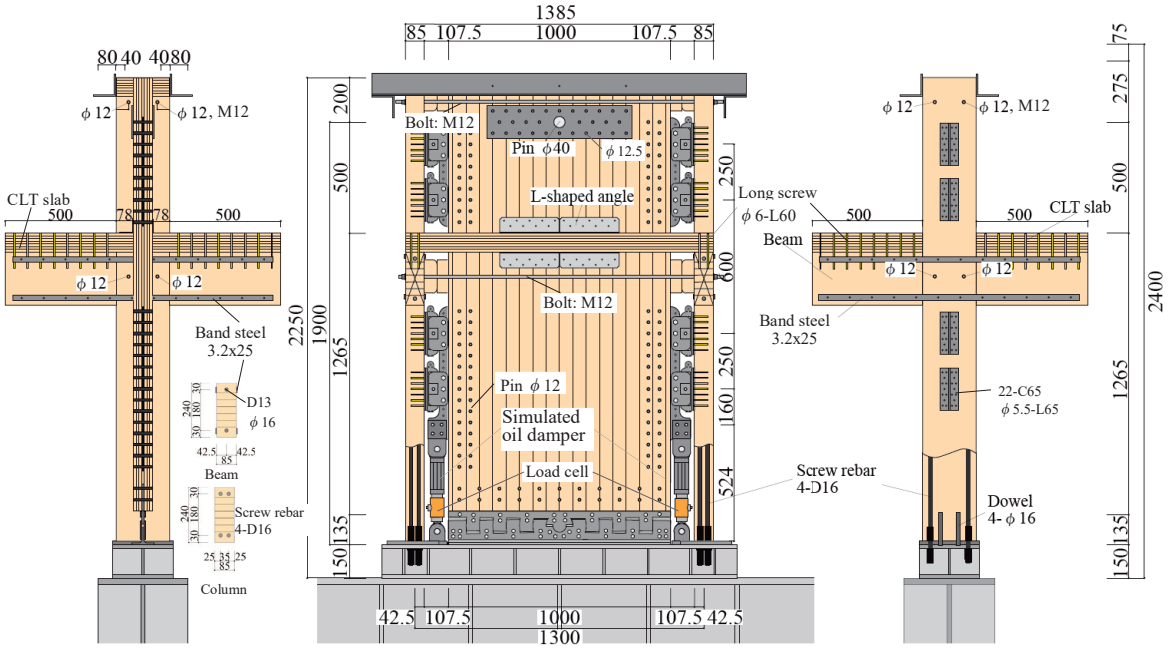

(a) Side view to CLT (b) Front (c) Side view to column

Figure 4: *Shape and dimensions of specimen*

centre of the thickness of the CLT and secured with drift pins. Part B is fixed to the side of the column with self-tapping screws.

Figure 3(a) shows a set-up for cyclic reversed loading test to investigate the frictional characteristics of the damper. In the damper, friction force and energy dissipation generate on two sliding surfaces between web of Part B and ultra-high-strength aluminium plate/ Part C. The aluminium plate is fixed to the splice plate using sand blast. The friction force-deformation relationship is shown in Figure 3(b)-(e). The friction force can be assumed to be 1/2 of the vertical load F. Deformation as horizontal axis in Figure 3(c) is the sliding deformation of the aluminium plate, which means that the initial stiffness is higher than others and there is little slackness. The skeleton curve of the relationship can be seen such as a tri-linear curve and not an inverted S shape curve. Except Figure 3(c), the curves have an inverted S-shaped loop shape with initial slackness caused by clearance around the drift pin or the screw. This characteristic was anxious to lead to a deterioration in horizontal shear force-drift relationship of the shear wall.

4 LOADING TEST OF SHEAR WALL

4.1 SPECIMEN

Figure 4 shows configuration of specimen, which was scaled at 40% and modelled as a range from the first floor to center of the second story height in frame planned such as one CLT panel was to be fitted in one span in the three-story frame consisting of steel rebar-timber composite columns and Glulam timber beams.

The column was rectangular in cross section and made of steel bar-timber composite member, which was selected to be in the weak axis direction of the column in loading direction. CLT panel and the columns were connected by

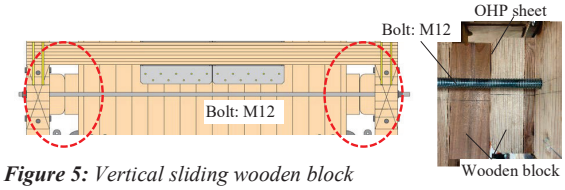

Figure 5: *Vertical sliding wooden block*

the friction damper mentioned in Chapter 3. No beam was employed to connect the left column and the right column. However, as shown in Figure 5, a pair wooden block was fixed to the column between the column and the CLT panel with tapping screws so that the interface of the wooden blocks could allow vertical sliding by being inserted a polyethylene terephthalate sheet. This prevents space between the columns and the CLT panel from closing, and separation between those is prevented by penetrating two long bolts through the columns on both sides and tightening those with washers and nuts.

This connectoin method is planned to be done at each floor, but in this specimen, it was also done near the top loading height.

Bottom of the CLT wall was connected to H-shaped steel flange as foundation by two pair-rotational shear key plates. However, in actual buildings, column bottom is planned to be anchored to reinforced concrete foundation by inserting column rebar into its ducts for the rebar and then grouting into the ducts.

Orthogonal beams were connected by glued-in-rod to the columns. The orthogonal beams were also made of steel bar-timber composite member. The second floor was made of the same CLT as the CLT wall and was connected to the CLT wall with L-shaped hardware joint. This was designed such that shear force could be transmitted from floor to wall. Two CLT slabs were connected by self-tapping screw to the orthogonal beams.

https://doi.org/10.52202/069179-0451

4.2 DETAILS OF SPECIMEN

4.2.1 Cross laminated timber (CLT)

The CLT had 84 mm thickness and consisted of 5 layers of 7 plies with lamina thickness of 12 mm which was width haggled. The strength grade was in accordance with cedar M60B of Japanese Agricultural Standard (JAS).

4.2.2 Column

The column adhered to cedar Glulam timber of E65F225 of JAS. Rebar was screw rebar with nominal diameter of D16 and yield strength level of SD390. The area ratio of tensile bars to column cross-section was 1.94%, and the ratio of the total rebars was 3.88%.

4.2.3 Connection of column bottom

Figure 6 shows detail of column bottom. The screw rebar coupler cut in 1/2 of the lengthwise direction was used as a nut. Nut/A was tightened on the column side with a lock nut. A steel plate was secured by wood screw to basement of the column, and then four dowel holes were drilled to match hole in the steel plate and four dowels were inserted. The column basement was fixed by tightening the screw rebar with nut B by passing the screw rebar and the dowel to upper flange of the H-shaped steel foundation. The steel plate was fixed to the H-beam with high-tension bolts.

4.2.4 Friction damper

Figure 7 shows detail of friction damper. High-strength aluminium plates (thickness=3.0 mm) are placed on both sides of web of T-shaped angle steel such as makes the joint surface slid. The tension of PC steel bar pressing the sliding surface was measured with a strain gauge embedded in the PC-steel bar. Splice plate was blasted on its one side to prevent misalignment with the aluminium plate. In addition, high-strength bolt was used to tighten splice plate to steel plate inserted into CLT panel to form friction joint between the splice plate and the inserted plate. Figure 8 shows shape and dimension of the inserted steel plate into CLT side face. The drift pin was made of hardened steel rod of S45C by heat treatment with a diameter of 12 mm.

4.2.5 Rotating shear key plate

Figure 8 shows a rotational pair-shear key plate (thickness = 9.0 mm). It was made of mild steel of SS400 and cut by laser-cut machine controlled with computer. Figure 10 shows set-up for the rotational shear key plate which consists of upper comb plate and lower comb plate.

Figure 11 shows the process of assembling of rotational shear keys. Upper two shear plates are friction-joined with high-strength bolts to both sides of the steel plate inserted to CLT-wall's bottom. Lower two shear plates are friction-joined with high-strength bolts to both sides of web of T-shaped angle steel secured to H-shaped steel foundation of reaction steel frame with high-strength bolts. The design of the pair shear key plate is based on magnitude of shear force and rotation angles to be allowed. The shear capacity of CLT wall of this specimen in design is 173 kN on the basis of its nominal shear strength and horizontal cross-section area considered wood ducts, and the pair-shear key plate can transmit shear force of approximately 1221 kN (= 9 x 1000/2 x 235/$\sqrt{3}$ x 2). Rotation angles of up to 3.3 x 10^{-2} rad. is to be allowable.

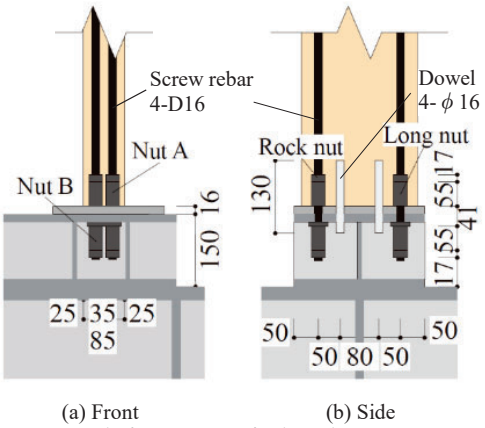

Figure 6: *Detail of connection of column bottom*

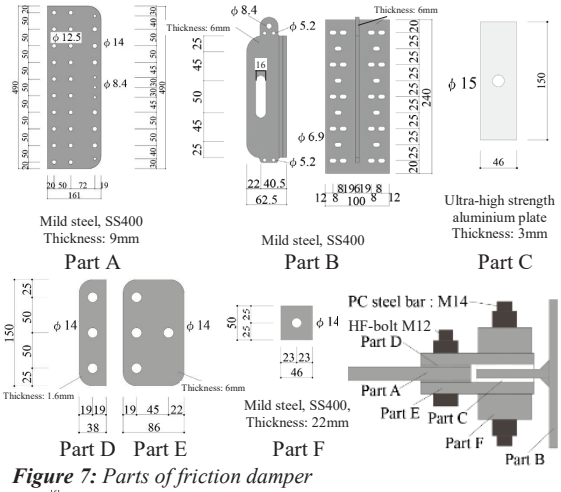

Figure 7: *Parts of friction damper*

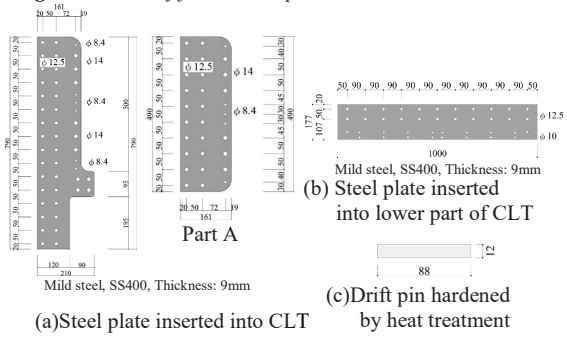

Figure 8: *Shape and dimensions of inserted steel plate*

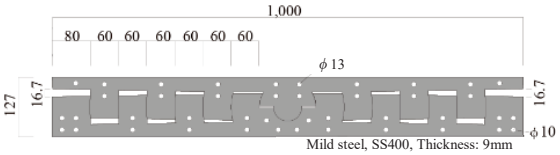

Figure 9: *Shape and dimensions of rotational shear key plate*

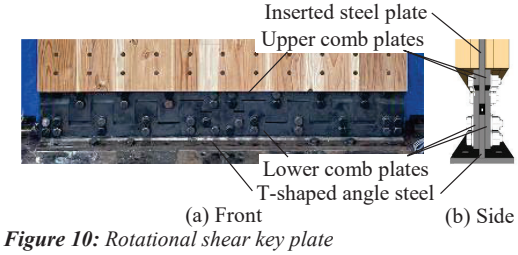

Figure 10: *Rotational shear key plate*

Photo 2: *Simulated oil damper adjusted to stiffness equivalent to oil damper up-down stiffness*

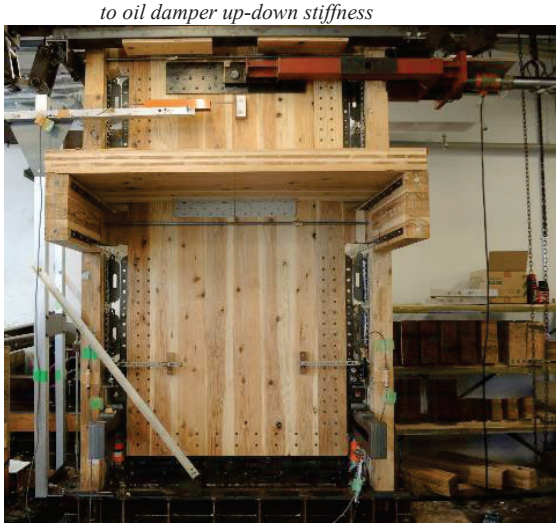

Photo 3: *set-up for loading*

4.3 LOADING

Figure 12 and Photo 3 show set-up for loading. H-beams of foundation were fastened to steel reaction frame with high-strength bolt, and repeated positive and negative cyclic horizontal force was applied at pin position at top of the CLT wall. No vertical load was applied to the columns. To prevent out-of-plane deformation of the top of the wall, two L-shaped steel beams sandwiched both side of the top of the wall, and the L-shaped steel beams and the reaction frame were connected by lateral braces. The lateral braces were joined so that the column heads were not restrained in loading direction. The loading protocol is shown in Figure 14. Orange colour indicates the force applied to check stiffness of specimen installed with each damper, and blue colour represents main protocol for seismic loading. The horizontal displacement at the top of the wall was controlled by deformation angle divided by 1691 mm of the height between the foundation and the displacement transducer. However, the initial 1-2 cycles were controlled by horizontal force.

4.4 MEASUREMENT

Figure 15 shows set-up for measurement of deformation and strain. The horizontal deformation of the wall was measured at the center of the wall width using displacement transducer attached to an aluminium frame fixed to the H-beam of the foundation, close to the height of the force point. Deformations of left and right dampers on the first story and the right damper on the second story, vertical up-down deformation of the CLT wall bottom, and the vertical deformation of CLT slab against the CLT wall were measured with displacement transducers.

Vertical axial strain and shear strain of CLT panel and vertical axial strain of timber near column bottom were measured with foil strain gauge (measuring length: 60 mm, long-term period measurement specification).

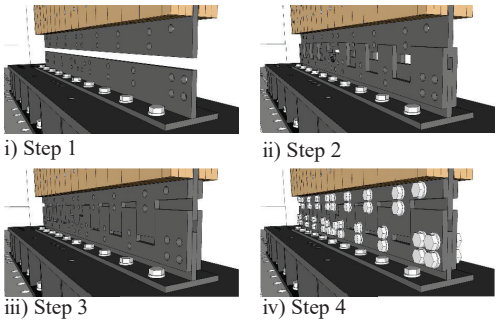

Figure 11: *Process of assembling of rotational shear key plates*

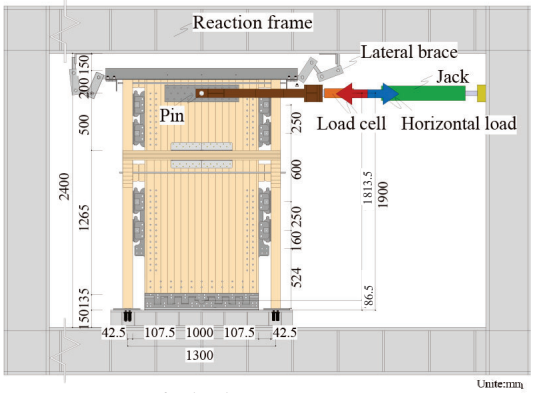

Figure 12: *Set-up for loading*

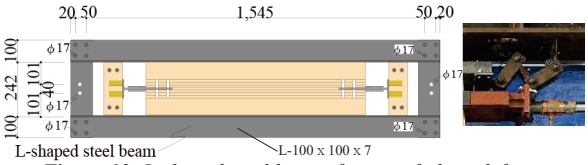

Figure 13: *L-shaped steel beams for out-of-plane deformation prevention*

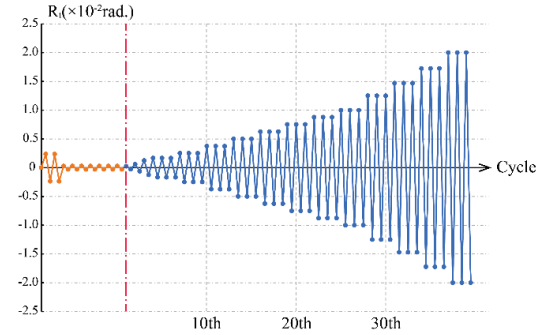

Figure 14: *Target displacement protocol for lateral loading*

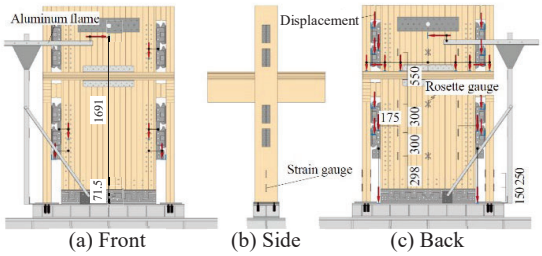

Figure 15: *Set-up for displacement and strain*

https://doi.org/10.52202/069179-0451

5 EXPERIMENTAL RESULTS

5.1 HORIZONTAL LOAD-HORIZONTAL DISPLACEMENT ANGLE RELATIONSHIP

Figure 17 shows horizontal force - deformation angle relationship. The deformation angle was calculated by dividing average horizontal displacement of the front and back near loading point by height of the displacement meter (1691 mm).

Horizontal force applied as reversed cyclic loading from the 4th cycle, experiencing each target deformation angle three times. The three cycles were observed to follow almost the same loop until the final deformation, and the cyclic loading did not cause any decrease in load capacity. The loops until the 30th cycle is shown in red and loops after the 30th cycle is shown in blue. Owing to loosening of the high-strength bolts of two splice plate of one friction damper connected to the top of wall from the 13th cycle to the 30th cycle, the relationship became loops such as it stiffs again after yielding.

This reason is considered that the stiffness is increased when the damper rotates owing to the loosening and the high-strength bolts strikes the side of hole in the splice plate and the inserted steel plate. After unloading at the time of recognizing the rotation of the splice plate, the friction damper was returned to be vertical and then the high-strength bolts were tightened.

Average shear stress obtained by dividing the maximum horizontal force of +110.4kN and -105.9kN at +1/50 rad. by area of horizontal cross section of CLT panel was 1.28 N/mm2. The average of those forces was 62% of shear capacity of the CLT wall bottom considering the deficiency by the drift pint and the inserted steel plate. As it may be possible to increase the horizontal loading capacity by increasing the tension of the PC steel bar in the friction damper, next work is going to reveal behaviour of the shear wall subjected to higher load levels by increasing the tension.

5.2 BEHAVIOR OF DAMPER

Figure 18 shows relationship of vertical shear force Q_D per a damper and sliding deformation δs between the inserted steel plate and the T-shaped angle steel. Q_D was calculated by the following Equation (1).

$$F \cdot h = 4 \cdot Q_D \cdot \ell \quad (1)$$

where F is horizontal force; h is height (1813.5mm) of the force point from rotational center of the rotational shear key; ℓ is horizontal distance (1100 mm) between the right damper and the left damper.

At first, the right-first damper on the lowest height from the bottom slid and yielded at -16.52kN in the fourth cycle; next, the right-third damper was done at -21.93kN in the seventh cycle; the left-first damper was done at -23.95kN in the tenth cycle, as well as the right-first damper.

As well as the horizontal force - deformation angle relationship, the relationship of damper was observed to

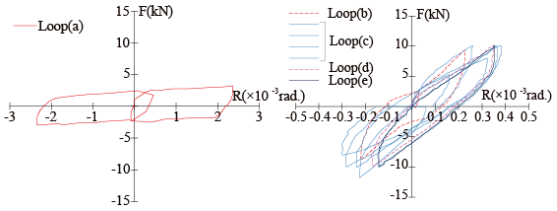

(a) Loop at step adding only rotational shear-key plate (b) Loops at steps adding each damper

Figure 16: *Lateral force-deformation angle Relationship*

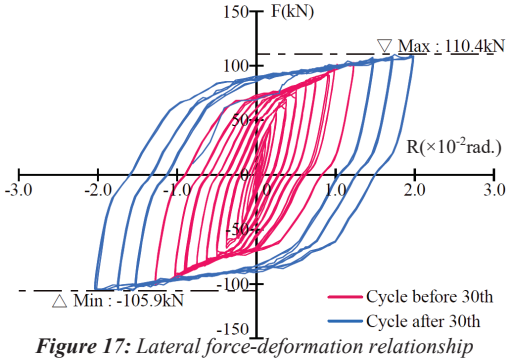

Figure 17: *Lateral force-deformation relationship*

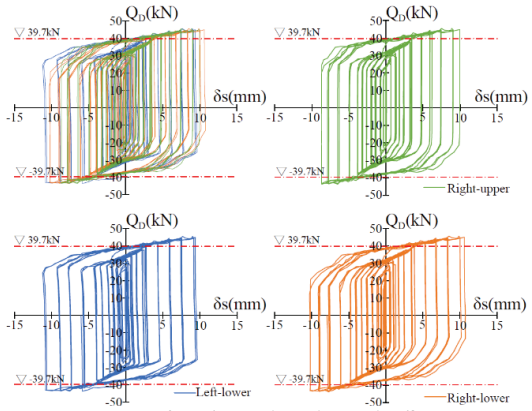

Figure 18: *Friction force/Q_D – slip relationship/δ between Part A –T-shaped angle steel*

be that of an increase in friction force after 1/68 rad. was observed. The maximum of sliding deformation of dampers during the final cycle of loading was+10.75 mm for the right-first damper; -11.22 mm for the left first damper; +9.97 mm for right third damper. The deformation of damper at higher position tended to be smaller, and the deformations of right and left dampers were to be close.

Figure 19 shows the relationship between tension change of the PC steel bar and sliding deformation in the damper. The target initial tension was selected to be 40.0 kN. The damper on the left side of the fourth row is considered to have loosened the PC steel bar due to the loosening of the high-strength bolt. Excluding this damper, the third row has the largest reduction, and the reduction became smaller as it approached the wall foot. It can be inferred that the frictional force might have been greater for the

https://doi.org/10.52202/069179-0451

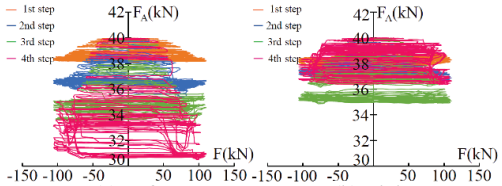

Figure 19: *Variation of tension in PC steel bar*

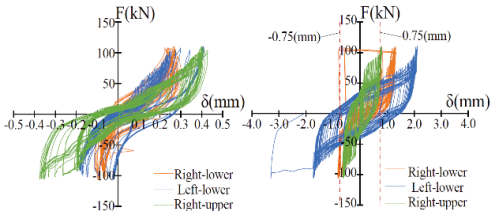

Figure 20: *Lateral force-slip deformation between CLT and Part A*

Figure 21: *Load – slip deformation between T-angle and column*

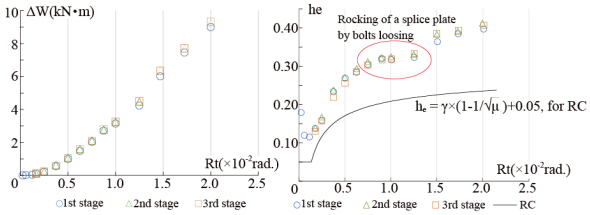

Figure 22: *Dissipation energy*

Figure 23: *Equivalent viscous damping factor/he*

right damper for the reason that the left damper has a greater reduction in tension than the right damper.

Figure 20 shows variation of sliding deformation of CLT and inserted steel plate against the horizontal force. It is an inverse S-shaped relationship with stiffness increasing from ±0.2 mm. The explanation of these is that after clearance of steel plate and its drift pin and clearance between drift pin and hole for itself in CLT closing, those resist each other. However, even maximums of sliding were negligible small.

Figure 21 shows variation of sliding deformation of the T-shaped angle steel against column. The maximum deformation in the final cycle was +1.333 mm at the right first damper; the left- first, +2.120 mm and the right third, +0.806 mm. A value of 0.75 mm sliding deformation is shown in the figure as a single vertical line, which roughly correspond clearance of hole in the T-angle steel and the neck of taping-screw. This also can be explained as clearance of those might have closed.

5.3 ENERGY DISSIPATION

Figure 22 shows variation of amount of energy dissipated by loops of each target deformation angle.

Although amount of energy at the same target deformation angle increased slightly in the second and third cycles compared to the first cycle, there was little difference in the amount, and there was no degradation of absorbed energy owing to the repetitive loading.

Figure 23 shows variation of the equivalent viscous damping constant he. The value calculated for reinforced concrete structure are represented by solid black lines.

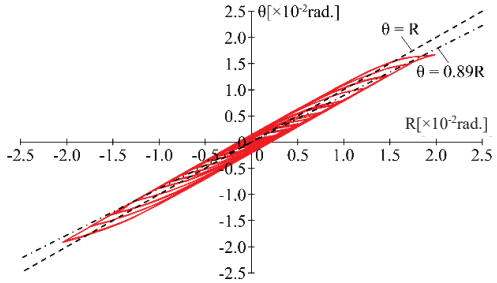

Figure 24: *Rotation angle of CLT– deformation angle relationship*

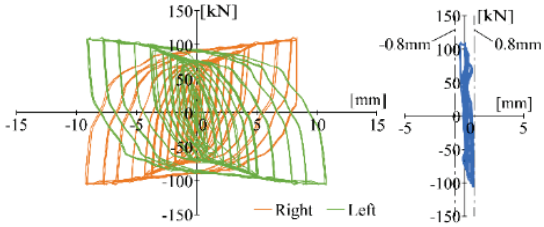

Figure 25: *Lateral force – vertical deformation of wall bottom relationship*

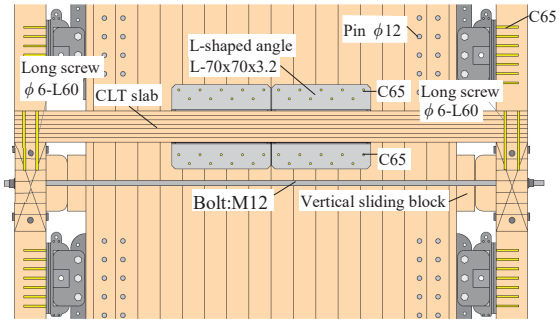

Figure 26: *Connection of CLT floor and CLT wall*

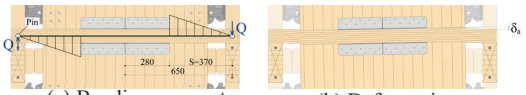

Figure 27: *Condition of CLT slab as CLT wall rotating*

This shear wall exhibited extremely high energy dissipation performance compared to RC, with performance of more than 10% from the initial deformation level and 40% at 1/50 rad.

5.4 WALL BOTTOM ROTATION

As shown in Figure 15, vertical displacements of CLT wall against the H-shaped steel of the foundation were measured on both left-hand and right-hand of the wall, by using transducers fixed to the lowest steel plate inserted into the CLT. Figure 24 shows variation of rotation angle of the CLT bottom calculated from the displacement, compared to the displacement angle as shear wall, i.e., drift. The rotation angle accounts for approximately 90% of the drift. Figure 25(a) shows variation of up-down displacements versus shear force. Figure 25(b) shows variation in the sum of two displacements at each side. This sum means vertical elongation at the rotation center of the rotating shear plate. Even when the drift increased up to 1/50 rad, the sum was less than ±0.8mm. This

https://doi.org/10.52202/069179-0451

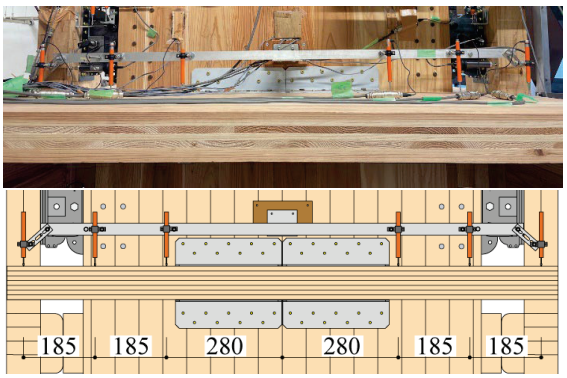

Figure 28: *Set-up for displacement*

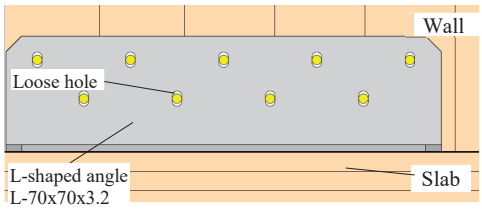

Figure 29: *Rotation-allowing angle steel*

demonstrates that the rotational shear key might have hardly elongated in vertically direction. This suggests that the left-hand dampers and the right-hand dampers might have slid as well, that sum of damper friction forces at each side might have been approximately same, and that the rotational shear key might not have been subjected to great tensile force in vertical.

5.5 VERTICAL DEFORMATION AND DAMAGE OF CLT SLAB

Figure 28 shows setup for measuring vertical displacement of the slab. An aluminium angle with displacement transducers attached were fixed to the CLT wall. The deformation measured is vertical deformation of the slab perpendicular to the aluminium angle.

The vertical deformation of the slab at each measured position against horizontal line passing through the fixed position of the aluminium angle can be approximated by the following Equation (2).

$$y_i = x_i \cdot \theta - \delta_i \quad (2)$$

where y_i and x_i are referred to Figure 30; θ is drift; δ_i is displacement of the transducer.

Figure 30 shows the distribution of the vertical deformation of the slab at a drift of +1/50 rad. The one dot chain line represents an inclination of drift=1/50 rad. This can be regarded as the inclination of the aluminium angle to which the displacement transducers were fixed. Vertical displacements of top surface of the slab can be calculated by using Equation (2), a distribution of which is shown by red solid line.

Even at the positions of the left and right boundaries of the L-shaped angle steel joint, values of the red line are different from those of the one dot chain line.

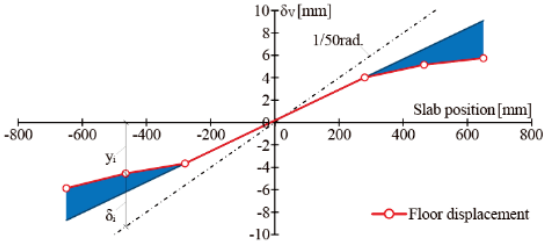

Figure 30: *Vertical displacement of floor*

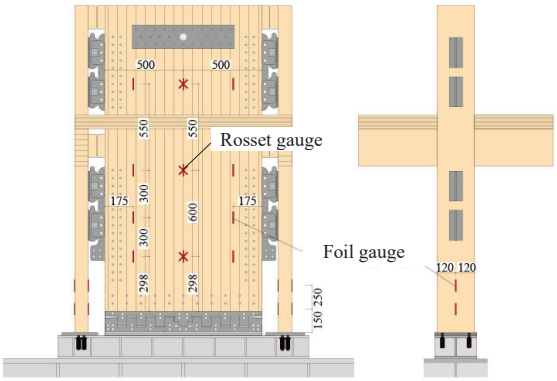

Figure 31: *Set-up for measurement of strain gauge*

This means that sliding deformation occurs between the CLT wall and the CLT slab over range of the angle steel joint. This may result from clearance between the screw holes and screw diameters at the joining angles and torsional deformation between the wall and the slab. The extent that the slab is deformed within range except the angle steel joint can be regarded as blue areas.

If the deformation of the slab is less than allowable value, no damage is expected to occur. The maximum values at drift=1/50. were 2.87 mm on the left side and 3.35 mm on the right side. In this experiment, the slab was not damaged even when the deformation reached 1/50 rad. This argues that this proposed system can significantly absorb the vertical deformation between column and wall, preventing the slab damage.

In the future, it is necessary to develop a method to estimate the deformation and damage deformation of slabs.

5.5.1 ROTATION-ALLOWING ANGLE STEEL

However, it is considered difficult to quantitatively estimate and design those factors. If the screw holes on the wall side of the angle steel are made vertical long holes as shown in Figure 29 so that the rotation of the wall is not restrained at the joint surface between the angle and the wall, the rotation of CLT wall and the vertical deformation caused by the rotation of wall bottom can be absorbed and the damage of CLT slab can be prevented, with transmitting transverse shear force by earthquake motion. Next experiment is planned to adopt the modified angle steel with the long holes.

https://doi.org/10.52202/069179-0451

5.6 SHEAR FORCE OF COLUMN

As shown in Figure 31, column strain was measured using foil gauges. Bending moment of column at each height position can be calculated by multiplying cross-sectional secondary moment of column by its curvature which is calculated using the strain of the foil gauge, as well known[3,4]. Shear force of column can be also calculated as gradient of two bending moments of lower and higher positions of the columns.

In the calculation, it was assumed that Young's modulus of timber is 6500N/mm^2 and that of rebar is 2.05x10^5 N/mm^2, which are nominal values of each. Figure 32 shows shear force vs drift relationship for the columns, comparing the horizontal force of the shear wall. The left and right columns resisted elastically up to 1/50 rad. At 1/50 rad. the positive force on the left column reached 9.5% of the horizontal force, and the negative force on the right column did 7.2%.

5.7 VERTICAL FORCE ON ROTATIONAL SHEAR KEY PLATE

Axial force of column can be calculated from strain of the strain gauges as well as bending moment. Figure 33 shows variation of sum of axial forces of the left and right columns. The sum must have been resisted by the rotational shear key plate. Although there is possibly some error because of Young's modulus of timber assumed as the nominal value, the sum at 1/50rad. is 6.6% of the column axial force calculated from the maximum horizontal load, which is extremely small. From this result, also, it can be seemed that the left and right friction dampers might have slid in good balance.

5.8 SHEAR STRESS-STRAIN RELATIONSHIP OF CLT WALL

As shown in Figure 31, shear strain was measured at three different heights by a rosette gauge (measuring length: 60 mm). Figure 34 shows average shear stress-shear strain relationship. Shear stress was defined as horizontal force divided by horizontal cross-sectional area of CLT wall. Shear strain was calculated from diagonal strain for simplicity; Figure 34(a) shows those up to initial ±3 cycles. Slope of the stiffness at the loop is shown by single-dotted line. The slope is the shear modulus G_W. Figure 34(b) shows those up to the final cycle. The plastic strain is found to be larger in upper part of the wall. This reason cannot have been explained at this time.

The shear modulus of CLT is, in general, 300-500 N/mm^2, but this experimental value is 3.0-4.0 times higher than the values. This is partly because of the assumption that shear forces of column was ignored and horizontal force was resisted by only CLT wall. However, as mentioned above, the shear forces of the column might have accounted for only 8.4% of the total load, so other factors may be responsible.

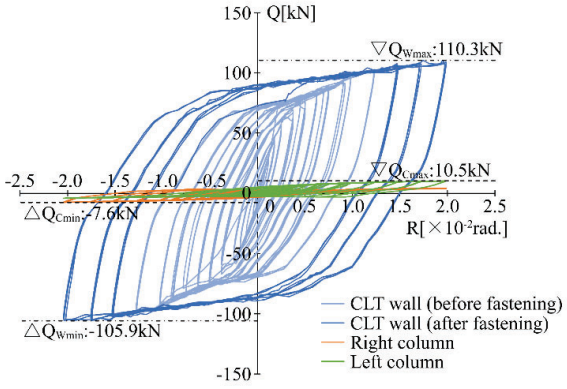

Figure 32: *Lateral shear force – displacement angle*

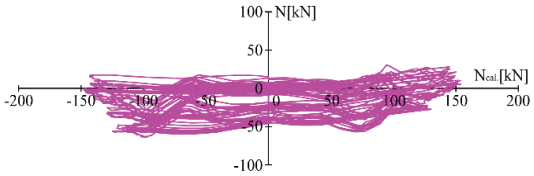

Figure 33: *Sum of axial forces of left-hand and right-hand columns calculated from strain gauge measurings - axial force of column calculated from lateral force relationship*

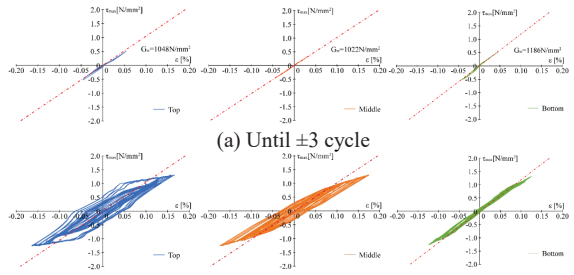

(a) Until ±3 cycle

(b) Until final

Figure 34: *Shear stress – shear strain relationship*

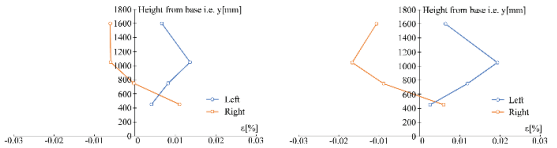

(a) +1/100rad. (b) +1/50rad.

Figure 35: *Distribution of vertical strain of CLT wall by bending*

5.9 DISTRIBUTION OF BENDING MOMENT OF CLT WALL

As shown in Figure 35, vertical axial strain of the CLT wall was measured at four heights with a foil strain gauge (measuring length: 60 mm). Strain values were extremely small, 0.019% at even maximum. Those cannot be analysed in detail considering the variation of wood, but those of the left side indicate tensile strain and those of the right-side do compressive strain. These results are the exact opposite against moment by horizontal force F under positive load. On the other hand, the strains near the rotational shear key and near the loading point will be smaller.

This can be explained as those positions are pins and bending moment is zero. These results can be considered

https://doi.org/10.52202/069179-0451

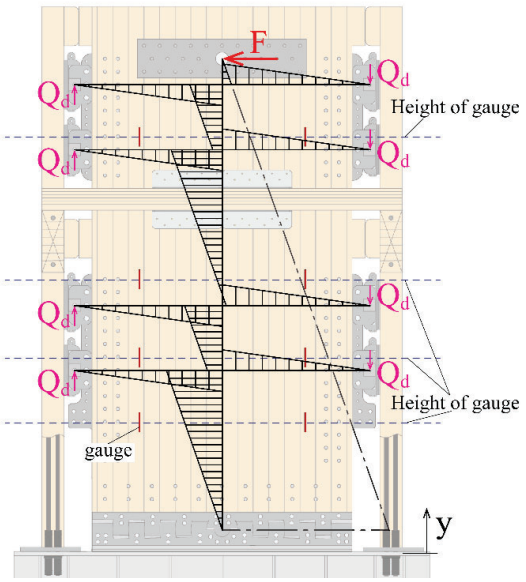

Figure 36: *Bending moment diagram for CLT wall*

to correspond to the distribution of bending moments in the CLT wall shown in Figure 36.

Moment by the horizontal force increases linearly as its height approaches the rotational shear key, as shown in one dot line, but bending moment of the CLT wall hardly increases because vertical friction force of each damper causes bending back. If shear force of columns is ignored because of it being small, horizontal shear force of the CLT wall can be considered constant regardless of height. Thereby, aspect of bending moment distribution of the CLT wall can be captured by assuming that the CLT wall bottom is pin. The heights of each strain gauge are represented by horizontal broken line. The left side is tensile, and the right side is compressive, corresponding to results of the strain in Figure 35.

These results demonstrate that the columns act as flange of wall and its CLT dose as web, similarly to H-shaped steel and that the columns resist against the bending moment of shear wall and the CLT wall dose almost against only the shear force. One of features of this shear wall is that the bottom of the CLT wall is connected to the foundation using rotational shear key plate, which significantly reduces bending moment of the CLT wall and perfectly suppresses damage of the CLT wall. The result of strain mentioned here is one of events supporting the features.

6 SUMMARY

In this paper, we proposed a shear wall system in which CLT panels are incorporated into a rigid-frame structure of steel bar-timber composite members, which authors have been developing, and revealed mechanical characteristic of the shear wall subjected to reversed cyclic lateral loading by a specimen scaled as 40%. The results are summarized as follows.

i) A friction damper so as to be installed between the CLT wall and the column and a connection method were proposed, and then it was confirmed that the damper can be easily joined. Although yield capacity of the damper increased with amount of its sliding deformation and the number of loading iterations, the capacity gradually converged to a constant value as the deformation increasing. Sliding deformation occurred in the joint between the damper and the CLT wall and in the joint between the damper and the column owing to clearance of holes in the drift pin or holes in self-taping screw, but the amount of deformation was almost negligible in the deformation of the shear wall.

ii) The rotational shear key plate was proposed to transmit shear force as the bottom of the CLT wall rotating, and it was confirmed that the plate could be easily joined to the CLT wall and that the incorporated CLT-shear wall allowed the rotation angle as planned.

iii) The shear wall yielded by sliding of friction damper at approximately 1/400 rad., and then produced elastoplastic history loops that generated extremely abundant energy dissipation and hardly degraded with repetitive loading.

iv) The maximum horizontal force in this loading test was 110.3 kN at 1/50 rad. This was 1.31 N/mm^2 at the average shear stress of CLT wall, which was 1.72 N/mm^2 when considering deficiency of joint drift pins and inserted steel plates at the wall bottom.

v) No failures were observed up to 1/50 rad. in this specimen by incorporating friction dampers and a rotational shear key plate and by making the best use of the steel bar-timber composite columns of flame.

vi) As it may be possible to increase the horizontal capacity of the shear wall by increasing tension of the PC steel bars, next work is going to reveal behaviour of the shear wall subjected to higher load levels by increasing the tension.

ACKNOWLEDGEMENT

This project was funded by Grant-in-Aid for Research-A in Japan and its experiment was conducted by all staffs of Shioya's laboratory. The authors gratefully acknowledge their work.

REFERENCES

[1] K. Nagano, et al.: Experiment of a new connection between column and beam producing high-energy dissipation and re-centering, Santiago, WCTE 2021.

[2] Francesco Sarti, et al.: Design and testing of post-tensioned timber wall systems, Quebec City, WCTE 2014.

[3] Kazuya Mori, Shinichi Shioya: Stiffness and strength of full-scale steel bar-timber composite beams with comparative small-depth, Santiago, WCTE 2021

[4] M. Mukai, Takao Ohota, Kazuya Mori, Riko Kawasaki, Shinichi Shioya: Horizontal - loading test of steel bar - timber composite column for mid-rise building, Santiago, WCTE 2021

[5] Kazuya Mori, Shinichi Shioya: Stiffness and strength of full-scale steel bar-timber composite beams with comparative small-depth, Santiago, WCTE 2021